Clinics in Oncology

Research Article
Published: 09 May, 2019

Molecular Imaging of RAGE Expression in Human Glioblastoma

*Yared Tekabe[1], Jordan Johnson[1], Qing Li[1], Rashmi Ray[2], Vivek Rai[2], Jerry Kokoshka[3] and Lynne L Johnson[1]**

[1]Department of Medicine, Columbia University Medical Center, USA

[2]Department of Biotechnology, Institute of Life Sciences, India

[3]Department of Technology Ventures, Columbia University, USA

Abstract

Introduction: The binding of Receptor for Advanced Glycation Endproducts (RAGE) and its ligands stimulate inflammation and angiogenesis and thereby contribute to tumor growth and metastasis. We developed an anti-RAGE antibody with good target binding and blocking properties. We tested the hypothesis that uptake of the radiolabeled antibody localizes and quantifies tumor RAGE expression in mice with implanted glioblastoma cell lines.

Methods: Inhibition of p-Akt and p-stat-3 was measured in U-87MG human glioblastoma cells by Western blot. For imaging, male athymic nude (J:NU) (n=13) mice, 5-6 weeks of age were injected subcutaneously in the right shoulder with U-87MG glioma cells (1×10^6). Four weeks later, mice were injected with 4.81 MBq ^{111}In-anti-RAGE F(ab')$_2$ (n=7) or nonspecific IgG F(ab')$_2$ (n=6). Mice were imaged on a small animal Single-Photon Emission Computed Tomographic (SPECT)/Computed Tomographic (CT) camera 48 h after injection (time based on blood pool clearance). After *in-vivo* imaging, the tumors were explanted, radioactivity counted, and sectioned for histological and immuno histochemical examination. Tumor activity from the scans was quantified using In Vivo Scope software.

Results: Anti-RAGE antibody showed blocking by Western blot analysis. All tumor-bearing mice injected with ^{111}In-anti-RAGE F(ab')$_2$ fragments showed focal areas of tracer uptake in the tumor. Quantitative tracer uptake in the tumor from scans showed significantly greater uptake of ^{111}In-anti-RAGE F(ab')$_2$ (1.44 ± 0.49) compared with ^{111}In-specific IgG F(ab')$_2$ (0.56 ± 0.25; P=0.006). *Ex-vivo* gamma counting showed greater tumor uptake of ^{111}In-anti-RAGE F(ab')$_2$ (3.92 ± 1% ID/g) compared with ^{111}In-nonspecific F(ab')$_2$ (1.21 ± 0.29; P<0.001). Dual immunofluorescence staining showed RAGE co-localization with GFAP-positive cells and macrophages and CD31-positive cells.

Conclusion: We showed anti-RAGE antibody with radiolabel can measure the extent of RAGE expression in glioblastoma and showed its property to block tumor.

Keywords: Glioblastoma; RAGE; SPECT/CT imaging

OPEN ACCESS

Correspondence:
Lynne L Johnson, Department of Medicine, Columbia University Medical Center, 630 W. 168th St, PH 10, room 203, New York NY 10032, USA, Tel: 212-305-4275; Fax: 212-305-4648; E-mail: lj2129@columbia.edu

Received Date: *13 Apr 2019*
Accepted Date: *06 May 2019*
Published Date: *09 May 2019*

Citation:
Tekabe Y, Johnson J, Li Q, Ray R, Rai V, Kokoshka J, et al. Molecular Imaging of RAGE Expression in Human Glioblastoma. Clin Oncol. 2019; 4: 1609.

Introduction

Receptor for Advanced Glycation Endproducts (RAGE) is a multiligand receptor of the immunoglobulin superfamily [1]. It was first identified as a cell surface receptor for Advanced Glycation Endproducts (AGEs) linking this receptor to diabetes, renal disease, and aging [2,3]. Further research revealed ligands that play important roles in inflammation and cancer including pro inflammatory cytokines S100 proteins and high-mobility group box 1 (HMGB1) proteins [4-7].

HMGB1 (amphoterin) is a nuclear non-histone chromatin-associated protein released from necrotic tumor cells, up regulated in cancer cells and implicated in tumor growth and metastasis including invasion and migration of invasive gliomas [8]. In glioblastomas, RAGE is expressed on tumor cells, endothelial cells, stromal cells, and on tumor-associated macrophages comprising microglia and myeloid derived macrophages [9]. HMGB1 is released into the tumor micro-environment from necrotic tumor cells. Binding to RAGE activates downstream signaling pathways that stimulate cell proliferation, survival, and migration via increases in angiogenesis, inflammation, and reduced apoptosis. Blocking RAGE-amphoterin (HMGB1) signaling suppresses tumor growth and metastasis [10-12]. These observations make RAGE an important target for both imaging and

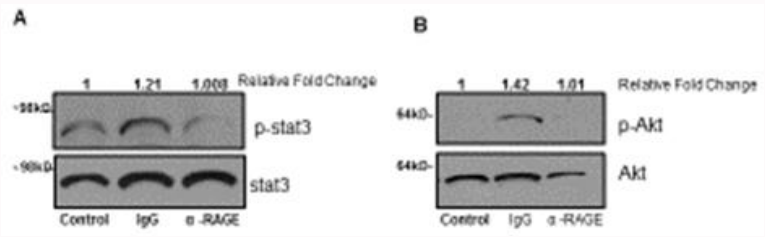

Figure 1: Levels of (A) phosphorylated/total stat3 and (B) p-Akt/Akt in U-87MG cells shown by western blotting upon stimulation with 10 µg/ml of AGEs for 20 min after treatment with 50 µg/ml of control IgG or anti-RAGE antibody fragments.

treatment.

In this study, we explored the application of an anti-RAGE antibody both as an *in-vivo* imaging agent in xengraft glioblastoma tumor implantations in mice and in cultured cells as a tumor suppressing agent.

Materials and Methods

All animal experiments were approved by the Institutional Animal Care and Use Committee of Columbia University.

Western blot analysis

U-87MG cells were maintained in DMEM medium supplemented with 10% Fetal Bovine Serum (FBS) and 1% penicillin/streptomycin (Gibco-Life Technologies, Grand Island, NY) in a 5% CO_2 incubator at 37°C. For experiments, cells were plated at a density of 1×10^5 cells/ml in 60 mm dish. Cells were serum starved overnight after they reached 70% to 80% confluency and next day were pre-treated with 50 µg/ml nonspecific IgG F(ab′)$_2$ or anti-RAGE F(ab′)$_2$ for one hour followed by treatment with 10 µg/ml of AGEs for 20 min. Tumor cells were lysed and total cellular lysates were immuno blotted and probed with RAGE, p-AKt, AKt, p-stat3 and stat3 antibodies. Proteins (35 µg) from cell lysates were denatured and resolved by 10% acrylamide gels and then transferred on nitrocellulose membrane. Membranes were blocked in 5% non-fat dry milk and incubated with primary antibodies- p-AKt, p-stat3, RAGE. HRP-conjugated anti-rabbit and anti-mouse IgG were used to identify sites of primary antibody binding. Membranes were stripped of bound primary antibodies and re-probed with total AKt and total stat3 antibodies.

Animals

Male nude (J:NU) mice (5 to 6 weeks of age) were purchased from The Jackson Laboratories (Indianapolis, IN). Mice were injected subcutaneously with human U-87MG glioblastoma cells (1×10^6 cells in 0.1 ml PBS) (n = 13) into the right shoulder. Tumor sizes were measured with calipers and the volume was calculated as (length × height × width x π)/6 [13]. Macroscopically, tumor-bearing mice developed palpable masses at the region of implantation with a mean tumor volume of 1245 ± 251 mm^3. Imaging experiments were performed 4-5 weeks after tumor injection. Tumor-bearing mice were injected with ^{111}In-anti-RAGE F(ab')$_2$ (n=7) or control nonspecific F(ab')$_2$ (n=6).

Radiotracer preparation

Murine monoclonal anti-RAGE antibody was developed as previously described [14]. For ^{111}In labeling, the antibody was fragmented into F(ab')$_2$ using pepsin digestion kit (Pierce, Grand Island, NY). Approximately 1 mg of the F(ab')$_2$ in 0.1 M NaHCO3 buffer (pH 8.2) was conjugated with 5 molar excess of Diethylene Triamine Pentaacetic Acid (DTPA; Sigma, St. Louis, MO). The reaction mixture was incubated at room temperature for 1 h in followed by overnight dialysis at 4°C in 0.25 M NH_4Ac (pH 5.5). To 10 µl (74-111 MBq) (2-3 mCi) of ^{111}In in 0.05 N HCl, 5 volumes of 0.1 M NH_4Ac (pH 5.5) was mixed and after 10 min, 50 µl (50 µg) of DTPA conjugated anti-RAGE F(ab')$_2$ was added. The reaction mixture was incubated at room temperature for 45 min. The ^{111}In labeled antibody fragments were separated from free ^{111}In using PD 10 column pre-equilibrated with 0.1 M NH4Ac (pH 6). The mean specific activity was about 36.4 MBq/µg of protein, and the mean radio purity was 98.7 ± 0.35% by Instant Thin-Layer Chromatography (ITLC).

In-vivo imaging

For imaging RAGE expression in human glioblastoma, ^{111}In-anti-RAGE F(ab')$_2$ (4.88 ± 0.129 MBq) was injected via the femoral vein catheter. Forty-eight h later, mice were imaged on a nano-SPECT/CT scanner (Bio scan, Washington DC). A tomogram (sequence of 2D side view of X-ray projections) was used to determine the axial scan range for SPECT and CT imaging. CT images were acquired with an integrated CT scanner using an X-ray tube at 45 kVp and an exposure time of 1000 ms per view. Following CT acquisition, helical SPECT scans were acquired using dual-headed detectors each outfitted with collimators with nine pinholes. The projection data were reconstructed by OSEM algorithm with subset and iteration number set to 16 and 8, respectively, and a voxel size of 300 µm and SPECT and CT datasets fused.

Image analyses

Using equal-size Regions Of Interest (ROIs) drawn in the trans axial plane, uptake of ^{111}In-anti-RAGE F(ab')$_2$ in the tumor was quantified in micro Curies as percentage injected dose (%ID). The imaging system is calibrated for absolute quantification using mouse-shaped phantoms filled with known levels of ^{111}In imaged with the same protocol used for the animal studies (In Vivo Scope software).

Gamma well counting

At completion of imaging, the mice were euthanized, the tumors excised and weighed and the radiotracer uptake was determined in a gamma well counter (Wallac Wizard 1470, PerkinElmer) and expressed as the percentage injected dose per gram (%ID/g) of tumor tissue. The radiotracer activity in the samples was corrected for background, decay time, and tissue weight.

Histopathology

The explanted tumors were fixed in 10% formalin for 24 h. Serial sections (5-µm-thick) from paraffin-embedded tumors were processed for Hematoxylin and Eosin (H&E) for morphological evaluation and immuno histochemical characterization. Serial sections were deparaffinized and rehydrated followed by quenching of endogenous

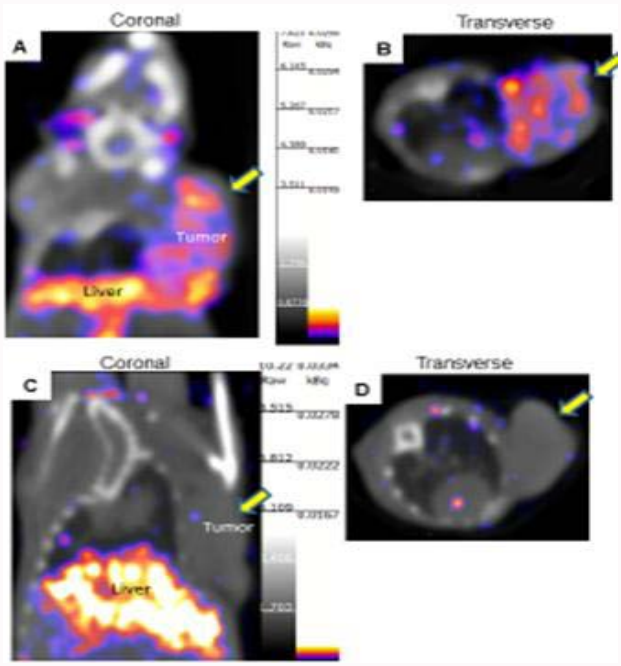

Figure 2: Representative coronal (left panels) and transverse (right panels) SPECT/CT images. There is focal uptake of ^{111}In-labeled anti-RAGE F(ab')$_2$ within the tumor (A,B) and no focal uptake of tracer is seen in a mouse injected with ^{111}In-nonspecific F(ab')$_2$ (C,D).

peroxidase activity with 0.3% hydrogen peroxide. Slides were then incubated overnight with primary antibody for RAGE (50 µg/ml; mouse anti-RAGE F(ab')$_2$). Slides were incubated for 30 min with biotinylated secondary antibodies. Sections were treated for 30 min with VECTASTAIN ABC reagent (Vector Laboratories, Burlingame, CA). Color reaction was visualized with 3',3'-diaminobenzidine (DAB substrate kit, Dako, Carpinteria, CA) and counterstained with Gill's hematoxylin solution.

Images were captured using a digital camera mounted on a Nikon microscope and analyzed using Image-Pro Plus software (Media Cybernetics Inc., Bethesda, MD).

Immunofluorescence

Dual fluorescent confocal microscopy studies were performed to identify RAGE positive cells. Tumor sections were subjected to immunofluorescence co-localization of RAGE with endothelial cells (CD31; 1:200; Dako), macrophages (Mac-3, 1:20; BD Pharmingen, San Diego, CA), and glial fibrillary acidic protein-positive cells

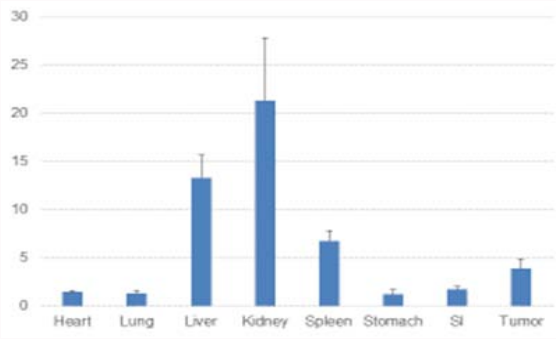

Figure 4: Bio distribution of ^{111}In-labeled anti-RAGE F(ab')$_2$ in tumor and non-tumor organs in male nude mice engrafted with U-87MG cells.

(GFAP;1:100; Novocastra Laboratories, UK) by overnight incubation at 4°C with the respective antisera. Sections were then incubated with conjugated fluorescent secondary antibodies (Texas Red anti-rabbit, fluorescein isothiocyanate anti-mouse and anti-rat; Vector Laboratories) at 1:200 at 4°C for 2 h. The images were examined using a fluorescence microscope (Nikon).

Statistical analyses

We compared the two groups using the Student t test. All statistical tests were two-tailed, with P<0.05 denoting significance.

Results

Western blot analysis

Western blot analysis demonstrated a marked reduction of p-stat3 and p-AKt (Ser473) in U-87MG cells pretreated with 30 µg/ml of anti-RAGE F(ab')$_2$ antibody compared to cells pretreated with control nonspecific F(ab')$_2$. Anti-RAGE F(ab')$_2$ pretreatment inhibited p-stat3 and p-AKt expression by 99.9% and 99.7%, respectively (Figure 1).

In-vivo imaging

SPECT/CT imaging of tumor bearing mice injected with ^{111}In-anti-RAGE F(ab')$_2$ showed heterogeneous distribution in the tumor (Figure 2A, 2B) top. An example from one control experiment is shown in Figure 2C, 2D (bottom). The quantitative accumulation of ^{111}In-anti-RAGE F(ab')$_2$ in the tumor from the scan (1.44 ± 0.49% ID) was significantly greater than the uptake in ^{111}In-nonspecific F(ab')$_2$ (0.5 ± 0.2% ID; P=0.006) (Figure 3A).

Ex-vivo gamma counting

The higher uptake of ^{111}In-anti-RAGE F(ab')$_2$ in the tumor was

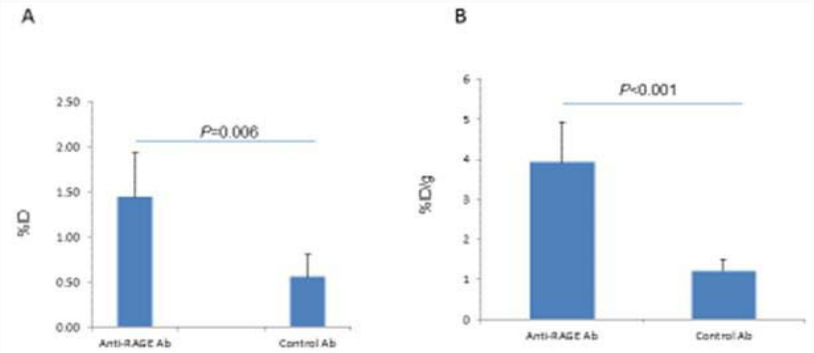

Figure 3: Quantitative tracer uptake from scan and gamma well counting. Radioactivity in the tumors shows significantly greater accumulations of ^{111}In-labeled anti-RAGE F(ab')$_2$ compared to ^{111}In-nonspecific F(ab')$_2$ from scan and gamma well counting; *P*=0.006 and *P*<0.001; respectively.

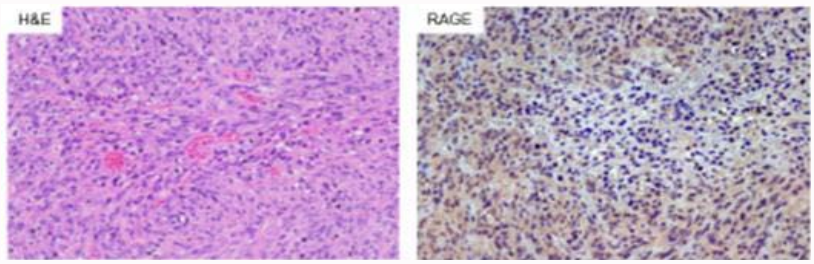

Figure 5: Histological view of U-87MG tumor sections. H&E stained section shows focal area of inflammation and necrosis. Immuno histochemical staining showed strong expression of RAGE.

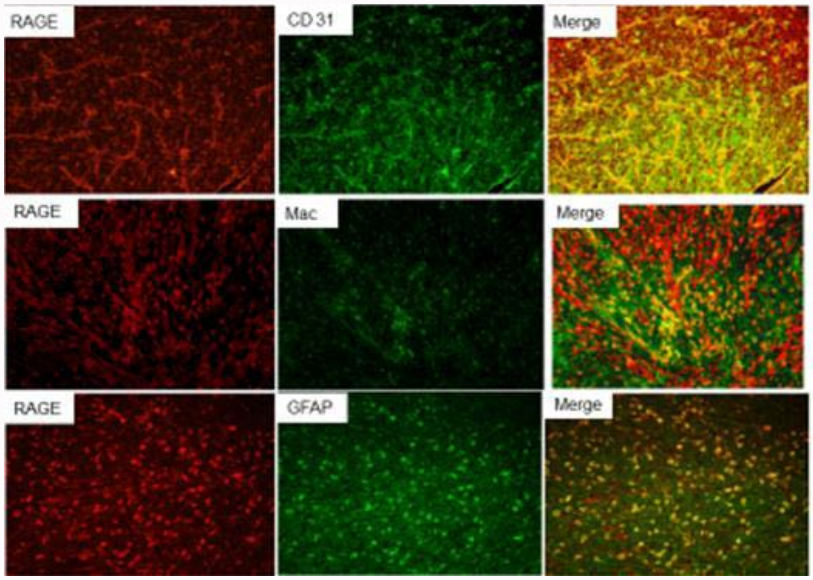

Figure 6: Dual fluorescent confocal microscopy of U-87MG tumor sections. Dual immuno fluorescent staining for RAGE and CD31-positive cells (top), for RAGE and macrophages (middle) and for RAGE and GFAP-positive cells (bottom). Colocalization is shown in the merged image (yellow). Magnification x 200.

confirmed by *ex-vivo* gamma counting (Figure 3B). There was a significant greater tumor uptake of ^{111}In-anti-RAGE F(ab')2 (3.92 ± 1% ID/g) compared with ^{111}In-nonspecific F(ab')$_2$ (1.22 ± 0.29; P<0.001).

Bio distribution of ^{111}In-anti-RAGE F(ab')$_2$ in non-target organs showed highest accumulation in the kidneys and liver (Figure 4).

Histopathology

H&E staining revealed richly cellular regions with foci of hemorrhage and necrosis (Figure 5). Immunohistochemical staining showed strong expression of RAGE. Dual immunofluorescence staining showed co-localization of RAGE with CD 31–positive cells, macrophages and GFAP-positive cells (Figure 6).

Discussion

This is the first report to document the feasibility of imaging RAGE in glioblastoma tumors in live animals using a radiolabeled anti-RAGE antibody. We observed focal, non-confluent uptake of the tracer in the tumor mass implanted in the shoulder region of nude mice. On immuno fluorescence, the RAGE staining localized to areas of CD31-positive cells, macrophages, and GFAP-positive cells.

The RAGE binding ligand that is highly expressed in glioblastoma is HMGB1. Intracellular signaling pathways initiated by RAGE/HMGB1 binding, promote proliferation and invasion of tumor cells via several pathways. In vitro binding studies have identified a cytoplasmic region of RAGE as an ERK docking site [8]. The ERK1/2 Mitogen-Activated Protein Kinase (MAPK) pathway is a central regulator of cell proliferation and activated in glioblastoma [8]. In addition, Rac 1 that is a major intracellular signaling pathway of RAGE plays a key role in HMGB1-stimulated migration of glioma cells. In glioma cells, the depletion of Rac 1 expression leads to decrease in cell migration and invasion [8].

Binding of RAGE to the ligand HMGB1 released during tumor necrosis triggers the invasion and migration of human glioma cells [8]. High-grade astrocytomas or glioblastomas are the most frequent and deadly primary intracranial tumors in adults. Malignant glioblastoma undergoing focal necrosis indicate a poor prognosis [15,16]. Tumors undergoing necrosis release HMGB1 into the micro-tumor environment. Binding of released HMGB1 to RAGE further stimulates expression of RAGE on tumor cells and on tumor-associated macrophages and through a positive forward feed-back loop promotes further inflammation leading to further necrosis [9]. This positive forward feedback cycle suggests that tumor aggressiveness may be measured by quantitative imaging of RAGE expression.

The role of RAGE to stimulate tumor angiogenesis in glioblastoma is more complicated and less well understood than inflammation. Blocking RAGE in non-aggressive bulky gliomas reduces number of micro vessels but shifts to production of large leaky vessels [9]. In invasive glioblastomas, blocking RAGE reduces angiogenesis but the

mechanism is not fully understood and may not depend on VEGF pathways but to the action of proteinases secreted by microglia and macrophages with angiogenic effects [9]. This would explain differences in role of RAGE in diabetes and cancer. In the former, increased RAGE expression in the vasculature inhibits the angiogenic response to hypoxia and contributes to diabetic vascular disease.

We developed a novel anti-RAGE antibody against a unique peptide sequence on the V-domain of RAGE designed to display immuno reactivity in mice, pigs, and humans [14]. We initially developed the antibody as an *in-vivo* imaging agent but subsequently found that it has blocking properties. We showed by Western blot blocking properties of the antibody in smooth muscle cells and in SKOV-3 ovarian cancer cells and in the current study extended our findings to include glioblastoma tumor cells [17]. In culture, cell viability of SKOV-3 paclitaxel-sensitive and paclitaxel-resistant SKOV-3 cells was reduced after treatment with anti-RAGE $F(ab')_2$ or with control $F(ab')_2$ [17-21].

Studies in glioma bearing mice using either RAGE knock-out transgenic mice or treatment with RAGE antagonists have shown beneficial effects including reduced inflammation, angiogenesis, and metastasis. In breast cancer, the RAGE blocking small molecule FPS-SM1 inhibited primary tumor growth and prevented metastases. These data suggests that blocking RAGE may be a therapeutic approach to treat some cancers including glioblastoma.

In summary, we have shown uptake of a radiolabeled anti-RAGE antibody in a focal pattern in human glioblastoma tumors implanted in nude mice. The focal areas of the antibody corresponded to areas of inflammation. RAGE targeting imaging may help identify hallmarks of tumor aggressiveness such as inflammatory necrosis that could be useful to plan treatment strategies. The blocking properties of the antibody suggest its potential as a therapeutic agent.

References

1. Bucciarelli LG, Wendt T, Rong L, Lalla E, Bowman HM, Goova MT, et al. RAGE is a multiligand receptor of the immunoglobulin superfamily: implications for homeostasis and chronic disease. Cell Mol Life Sci. 2002;59(7):1117-28.
2. Ramasamy R, Yan SF, D'Agati V, Schmidt AM. Receptor for Advanced Glycation Endproducts (RAGE): a formidable force in the pathogenesis of cardiovascular complications of diabetes and aging. Curr Mol Med. 2007;7(8):699-710.
3. Yan SF, Ramasamy R, Schmidt AM. Mechanisms of disease: advanced glycation endproducts and their receptor in inflammation and diabetes complications. Nat Clin Pract Endocrinol Metab. 2008;4(5):285-93.
4. Srikrishna G, Freeze HH. Endogenous damage-associated molecular pattern molecules at the crossroads of Inflammation and cancer. Neoplasia. 2009;11(7):615-28.
5. Sparvero LJ, Asufu-Adjei D, Kang R, Tang, Amin N, Im J, et al. RAGE (Receptor for advanced glycation endproducts), RAGE ligands, and their role in cancer and Inflammation. J Transl Med. 2009;7:17.
6. Rojas A, Figueroa H, Morales E. Fueling inflammation at tumor microenvironment: the role of multiligand/rage axis. Carcinogenesis. 2010;31(3):334-41.
7. Hoffman MA, Drury S, Fu C, Qu W, Taguchi A, Lu Y, et al. RAGE mediates a novel proinflammatory axis: a central cell surface receptor for S100/calgranulin polypeptides. Cell. 1999;97(7):889-901.
8. Bassi R, Giusanni P, Anelli V, Colleoni T, Pedrazzi M, Parone M, et al. HMGB1 as an authocrine stimulus in human T98G gliobastoma cells: role in cell growth and migration. J Neurooncol. 2008;87(1):23-33.
9. Chen X, Zhang L, Zhang IY, Liang J, Want H, Ouyang M, et al. RAGE expression in tumor-associated macrophages promotes angiogenesis in glioma. Cancer Res. 2014;74(24):7285-97.
10. Taguchi A, Blood DC, del Toro G, Canet A, Lee DC, Qu W, et al. Blockade of RAGE-amphoterin signaling suppresses tumour growth and metastases. Nature. 2000;405(6784):354-60.
11. Kwak T, Drews-Elger K, Ergonul A, Miller PC, Braley A, Hwang GH, et al. Targeting of RAGE-ligand signaling impairs breast cancer cell invasion and metastasis. Oncogene. 2017;36(11):1559-72.
12. Choi E, Oh J, Lee D, Lee J, Tan X, Kim M, et al. A tertiary-complex of a suicide gene, a RAGE-binding peptide, and polyethylenimine as a gene delivery system with anti-tumor and anti-angiogenic dual effects in glioblastoma. J Control Release. 2018;279:40-52.
13. Tomayoko MM, Reynolds CP. Determination of subcutaneous tumor size in athymic (nude) mice. Cancer Chemother Pharmacol. 1989;24(3):148-54.
14. Tekabe Y, Luma J, Einstein A, Sedlar M, Li Q, Schmidt AM, et al. A novel monoclonal antibody for RAGE-directed imaging identifies accelerated atherosclerosis in diabetes. J Nucl Med. 2010;51(1):92-7.
15. Louis DN, Ohgaki H, Wiestler OD, Cavenee WK, Burger PC, Jouvet A, et al. The 2007 who classification of tumours of the central nervous system. Acta Neuropathol. 2007;114(2):97-109.
16. Tysnes BB, Mahesparan R. Biological mechanisms of glioma invasion and potential therapeutic targets. J Neurooncol. 2001;53(2):129-47.
17. Tekabe Y, Li Q, Rodriquez K, Johnson J, Khaw BA, Kokoshka J, et al. Targeting RAGE expression in human ovarian cancer. Clin Oncol. 2016;1:1055.
18. Tekabe Y, Li Q, Rosario R, Sedlar M, Majewski S, Hudson BI, et al. Development of receptor for advanced glycation end-products directed imaging of atherosclerotic plaque in a murine model of spontaneous atherosclerosis. Circulation CV Imaging. 2008;1:212-9.
19. Johnson LL, Tekabe Y, Kollaros M, Eng G, Bhatia K, Li C, et al. Imaging RAGE expression in atherosclerotic plaques in hyperlipidemic pigs. EJNMMI research. 2014;4:26.
20. Tekabe Y, Kollaros M, Li Q, Zhang G, Li C, Schmidt AM, et al. Beneficial effect of glucose control on atherosclerosis progression in diabetic ApoE-/- mice: Shown by Rage directed imaging. Int J Mol Imaging. 2014;2014:695391.
21. Tekabe Y, Shen X, Luma J, Weisenberger D, Yan SF, Haubner R, et al. Imaging the effect of receptor for advanced glycation endproducts on angiogenic response to hindlimb ischemia in diabetes. EJNMMI Res. 2011;1(1):3.